ERDC/LAB TR-0X-X

Insert Name of ERDC
Laboratory or the Center

US Army Corps
of Engineers®
Engineer Research and
Development Center

ERDC
ENGINEER RESEARCH & DEVELOPMENT CENTER

Forecast-Informed Reservoir Operations

Assessing Quantitative Precipitation and Inflow Forecast Skill for Potential Forecast-Informed Reservoir Operations for Lake Mendocino

Rachel R. Weihs, David W. Reynolds, Robert Hartman, Scott L. Sellars, Daniel Kozlowski, F. Martin Ralph

April 2020

The U.S. Army Engineer Research and Development Center (ERDC) solves the nation's toughest engineering and environmental challenges. ERDC develops innovative solutions in civil and military engineering, geospatial sciences, water resources, and environmental sciences for the Army, the Department of Defense, civilian agencies, and our nation's public good. Find out more at www.erdc.usace.army.mil.

To search for other technical reports published by ERDC, visit the ERDC online library at http://acwc.sdp.sirsi.net/client/default.

Assessing Quantitative Precipitation and Inflow Forecast Skill for Potential Forecast-Informed Reservoir Operations for Lake Mendocino

Rachel R. Weihs[1], David W. Reynolds[2], Robert Hartman[3], Scott L. Sellars[4], Daniel Kozlowski[5], F. Martin Ralph[1]

1) Center for Western Weather and Water Extremes, Scripps Institution of Oceanography, University of California, San Diego
9500 Gilman Drive #0224
La Jolla, CA, 92093-0224

2) Cooperative Institute for Research in the Environmental Sciences,
University of Colorado,
Boulder, CO

3) Robert K. Hartman Consulting,
Sacramento, CA

4) Office of Advanced Cyberinfrastructure
National Science Foundation
2415 Eisenhower Ave,
Alexandria, VA 22314

5) NOAA National Weather Service, California-Nevada River Forecast Center
3319 El Camino Ave #228
Sacramento, CA, 95821

Final report

Prepared for U.S. Army Corps of Engineers

Washington, DC 20314-1000

Under Work Unit 33143

Monitored by Coastal and Hydraulics Laboratory
U.S. Army Engineer Research and Development Center
3909 Halls Ferry Road, Vicksburg, MS 39180-6199

Abstract

The Forecast-Informed Reservoir Operations (FIRO) program seeks to improve the management of reservoir water supply by incorporating weather forecast information when making decisions on conservation storage as well as pre-releases of water when encroaching on the flood control space. Potential FIRO is presented in context with northern California's Lake Mendocino Reservoir and Russian River watershed, a key water supply area susceptible to the variable cool-season weather and climate in California. The FIRO Assessment Framework is defined, where dam design criteria are identified and critical forecast lead-times to mitigate flooding concerns are determined for potential FIRO operations. First, lead-times are identified based on the time necessary to evacuate expected additional stored water in the flood pool prior to an expected precipitation event and the time necessary for this water to pass by vulnerable locations downstream. Next, precipitation and inflow forecasts from the California Nevada River Forecast Center are analyzed to determine resulting skill on timescales suitable for dam operations as well as for FIRO. Finally, extreme events in this area are identified using return period frequency characteristics and analyzed for trends according to mean areal precipitation magnitudes.

Contents

Preface

This study was conducted for the U.S. Army Corps of Engineers (USACE), Engineering Research and Development Center (ERDC) Coastal and Hydraulics Laboratory (CHL) under [[[Funding information from title page/Form 7]]]. The program manager was Dr. Cary A. Talbot.

This contract report was prepared by an interdisciplinary team from the Center for Western Weather and Water Extremes (CW3E) at Scripps Institution of Oceanography (SIO) University of California San Diego (UCSD), Cooperative Institute for Research in the Environmental Sciences (CIRES) in Boulder, CO, and the California-Nevada River Forecast Center (CNRFC) in Sacramento, CA. The Co-PI at CW3E was Mr. F. Martin Ralph. This work was funded by ERDC-CHL (Grant no. W912HZ-15-2-0019).

At the time of publication of this report, Dr. Hwai-Ping Cheng was Chief, Hydrologic Systems Branch; Dr. Cary A. Talbot was Chief, Flood and Storm Protection Division; and Dr. Julie D. Rosati was the Technical Director for Flood Risk Management. The Deputy Director of ERDC-CHL was Mr. Jeffrey R. Eckstein, and the Director was Dr. Ty V. Wamsley.

The paper was greatly improved by the comments from Mr. Stephen Turnbull and Mr. Charles Downer of ERDC-CHL, along with three anonymous reviewers. The authors express appreciation to Ms. Julie Kalansky of CW3E and Mr. Dan Gottas of NOAA Physical Sciences Division and Mr. Tim Coleman at the University of Colorado for help in data processing, and Mr. Tony Tullos of ERDC-CHL for manuscript preparation.

The Commander of ERDC was COL Teresa A. Schlosser, and the Director was Dr. David W. Pittman.

Figures and Tables

Figures

Tables

Unit Conversion Factors

Multiply	By	To Obtain
acre-feet	1,233.5	cubic meters
atmosphere (standard)	101.325	kilopascals
cubic feet	0.02831685	cubic meters
inches	0.0254	meters
quarts (U.S. liquid)	9.463529 E-04	cubic meters

1 Introduction

Reservoirs are authorized, funded, and constructed with the purpose of flood risk reduction, water supply storage, navigation, recreation, hydropower generation, and/or ecosystem sustainment. Guidelines and rules for operating the reservoir are created when the project is constructed and are periodically updated on an "as needed" basis. Over time, watershed changes can take place due to development, altered land use, increasing water demand, and climate change. In addition, new or altered regulatory practices can further affect changes to the function of the watershed system. The guidelines and objectives used to operate the watershed are, however, mainly based on the factors considered during the era of construction, and thus they may be out of date. Improvements in the understanding of changing watershed characteristics, along with advances made in the predictability of impactful weather and climate in susceptible watersheds, can be widely explored to help re-assess these potential benefits of modifying the pre-determined sets of objectives and goals for a given reservoir.

To this end, the Forecast-Informed Reservoir Operations, or FIRO (http://cw3e.ucsd.edu/FIRO/) project, seeks to use state-of-the-science weather and hydrologic forecasts, coupled with operational decision support tools, for retaining and releasing water from a reservoir, namely Lake Mendocino (see Section 2, Lake Mendocino and the Coyote Valley Dam), during an extreme weather and runoff event. FIRO seeks to add flexibility to decisions made by water resource engineers when considering holding or releasing water storage prior to an impending event (Miller 1996, Lund 1997, Biswas 2004, Hoff 2009, Ralph 2011, Leung 2009, Smith and Merenlender 2010, Lund 2015, Yang et al. 2015, 2016).

The goal of this research is to determine, based on the FIRO objectives, the time scales in which forecasts need to be evaluated to support FIRO-based operations (i.e. modification of water storage requirements) and evaluate the current forecast skills of quantitative precipitation forecasts (QPF) and inflow forecasts for a given reservoir with defined flood control, water supply, and ecological objectives. It is important to note that FIRO is a "non-structural" approach that has the potential to improve water supply reliability, flood protection, ecological benefits, and other project

outcomes. At the heart of FIRO is the ability to accurately forecast weather and hydrological events that could inform operational decisions on potential alternate management strategies. Those strategies ideally would result in additional flexibility when managing the reservoir. Specific reservoir design features and safe operational criteria play a key role in FIRO. Yet, at this time there is not a generally agreed upon framework for assessing reservoir characteristics and operations in the context of FIRO.

In this report, Section 1 outlines the FIRO assessment framework, in which the dam operational criteria and reservoir design elements are identified in terms of managing the reservoir and the downstream limitations to flow rates, travel times, and flood risk. The key criteria and limitations of the reservoir are then used as thresholds for evaluating the skill of forecasted hydrologic events in the watershed over the last two decades. These steps are vital in determining the viability of using forecasted precipitation information for the given watershed. Section 2 provides a background on Lake Mendocino (Lake Mendocino and the Coyote Valley Dam), the FIRO assessment framework (FIRO Background), and the current dam operating criteria are described in section 3. Section 4 describes a preliminary set of requirements as defined by the reservoir's Water Control Manual (WCM) and establishment of forecast lead-times based on the travel time of pre-releases made in advance of extreme precipitation events. Section 5 describes the results of the QPF and inflow verification during the cool season with respect to all observations and extreme events, and Section 6 contains a discussion with a summary of major conclusions.

2 Background, Data, and Methodology

Lake Mendocino and the Coyote Valley Dam

Lake Mendocino is a reservoir located near the headwaters along the East Fork of the Russian River watershed in Northern California, between two coastal mountain ranges (Figure 1). The Russian River basin is home to approximately 4.94×10^8 m^2 (122,000 acres) of agriculture, most of which is vineyards. In 1958, the U.S. Army Corps of Engineers (USACE) constructed the Coyote Valley Dam (CVD) to produce Lake Mendocino with a watershed of ~ 272 km^2. The USACE and Sonoma County Water Agency (SCWA) jointly operate the reservoir utilizing the Lake Mendocino Water Control Manual (WCM) (see Figure 3); the first being developed in 1959 and revised in 1986. CVD was designed for flood protection, water supply, irrigation, streamflow regulation for habitat protection, power and recreational use (WCM 1986). The WCM contains a "rule curve" that defines allowable water storage levels throughout the year (see Section 3). Given the era of the construction of the dam (1959), operations rules were engineered without the benefit of sophisticated numerical weather prediction and hydrologic model forecasts. This was entirely appropriate, as forecast skill was quite limited at the time, numerical weather prediction models were in their infancy, and global scale satellite observations were relatively non-existent (Benjamin et al. 2018). Over the last several decades, however, weather forecast skill has consistently improved (e.g. 40% increase in annual threat scores for 25.4 mm (1 inch) rainfall in 24-hrs between 1961 to 2017) to the point where it is integral to the operations of our modern day societal infrastructure, including aviation, power generation, construction, agriculture, health and safety (Benjamin et al 2018). While the WCM itself was updated in 1986, subsequent revisions have not altered the project's rule curve at Lake Mendocino.

Operations defined in the WCM include obtaining appropriate hydrologic and weather forecasts, determining what schedule the dam should be operated, computing hydrologic inflow/outflows/evaporation, and making subsequent releases/storage decisions. Actionable criteria for forecasted precipitation are 12.7mm [0.5 inch] 6h^{-1} and 25.4mm [1 inch] 24h^{-1}. This report contains the skill assessment of rainfall, and subsequent inflows, using modern forecast information in the context of those current

operations and how this assessment fairs with timescales needed to account for rule curve modifications under FIRO.

The Russian River's Mediterranean climate is characterized by cool-season wet period in which approximately 90% of its annual precipitation occurs between November and April of each year and large variability in annual precipitation from year to year (e.g. Opperman et al. 2005). Average annual precipitation over the Lake Mendocino watershed is 1079 mm (42.5 inches) but varies from 483 mm (19 inches) per year near the dam to as high as 2108 mm (83 inches) per year in the upper basin. Dettinger et al. (2011) showed that the difference between a wet year and a dry year in Northern California can be the occurrence, or lack of, a few major rain events. These major rain events often come in the form of atmospheric rivers (hereafter ARs) that are defined as narrow plumes of strong, low-level horizontal vapor transport (Ralph et al. 2004, Neiman et al. 2008a), which can impact the U.S. West Coast with heavy rain (Ralph et al. 2005, 2011, 2013; Leung and Qian 2009; Neiman 2008b, 2011, Smith et al. 2010, Dettinger et al. 2012, Ralph and Dettinger 2012; White et al. 2012, Sellars et al. 2015, Neiman et al. 2016). Ralph et al. (2006) showed that ARs accounted for 34 of the 39 floods along the Russian River between 1948-2005.

Forecasting extreme precipitation in this region is challenging given the complex topography and narrow plumes of moisture transport inside ARs (Olson et al. 1995, Cherubini et al. 2002, Charba et al. 2003, Ralph et al. 2010, Schumacher et al. 2010, Novak et al. 2014, Sukovich et al. 2014, Cordeira et al. 2017). Hydrological forecasts that integrate the precipitation forecasts have similar forecasting challenges (Franz et al. 2011, Pappenberger et al. 2011, Brown et al. 2014, Demargne et al. 2014). This paper presents a methodology for determining the forecasted precipitation and inflow skill at Lake Mendocino at time scales determined by the dam operating requirements and flood wave travel times.

Figure 1. U.S. West Coast terrain height (m, left) with an outline of the region of the Russian River Watershed and Lake Mendocino in Northern California. The region outlined in black is shown on the right where the green shaded area is the Russian River watershed, the dark blue line is the Russian River, the light blue region is Lake Mendocino, and the location of cities within the watershed are noted. All locations (except Santa Rosa) have a stream gauge along the Russian River.

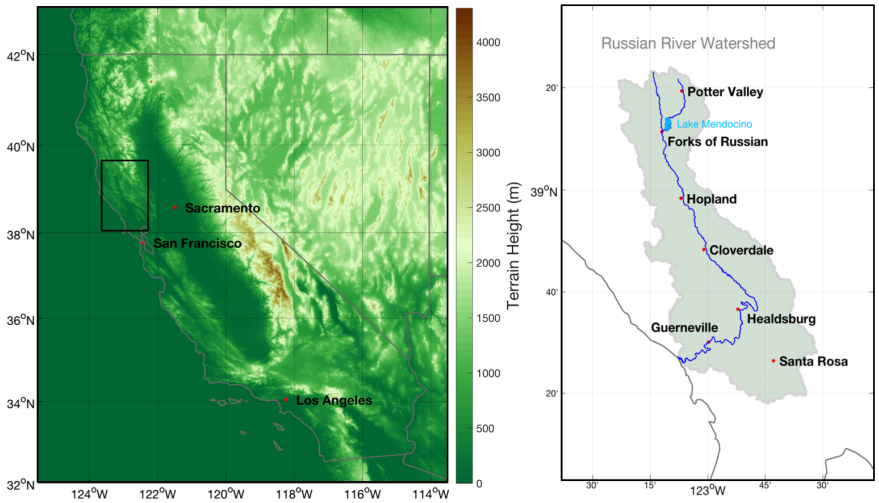

FIRO Background

The objective of FIRO is to provide tools and science that enable better management of reservoir water storage at Lake Mendocino by leveraging state-of-the-art forecast information. At the heart, FIRO has the ability to improve the water storage at Lake Mendocino at the end of the wet season by allowing currently allocated flood control space to be used as conservation storage when relatively insignificant precipitation is expected in a given forecast period. The tools and science applications also need to be developed with strategies that will not increase flood risk by using the defined ramping and release rates to pre-release stored water when flood control space is needed in advance of a more significant runoff event.

To evaluate the viability of FIRO to benefit the storage and flood risk capabilities of Lake Mendocino, this paper proposes a three-step process named “The FIRO Assessment Framework” (FIRO-AF), illustrated in Figure 2. The first step entails working closely with dam operators to select specific reservoir criteria used in operations, critical precipitation and inflow magnitudes, specific release rates and ramping rates for flood releases, emergency release criteria, downstream flow restrictions and flooding concerns, and potential storage. Step 2 includes a systematic assessment of quantitative precipitation forecasts (QPFs) followed by

inflow forecasts that address the key design elements and operational criteria found in Step 1. If either QPF or inflow forecasts lack sufficient skill, forecast improvements would need to take place before or as a part of a FIRO strategy for the reservoir of interest. The thresholds used herein are the sufficient forecast lead-time required for the release of additional (or excess) water stored (i.e., the FIRO proposed increase in water storage) in the flood pool in anticipation of a large runoff event that could lead to a spill or higher than desired releases and the length of time it takes for this water to pass all vulnerable locations downstream. The authors note that knowledge of the QPF and inflow forecast accuracy and skill is not, however, sufficient to suggest that FIRO may be effective for a reservoir. Ultimately, this becomes a function of the capacity of the flood pool, the magnitude of the runoff events it was engineered to accommodate, and the reduction in uncertainty provided by a skillful inflow forecast. This report will address Steps 1 and 2 of the FIRO-AF to determine the skill in precipitation and inflow on lead time scales related to dam operations, regulations, and impacts. Step 3 will be fully addressed in the project's Final Viability Assessment (FVA) that will include engineering as well as environmental impacts of a fully implemented FIRO.

Figure 2. FIRO Assessment Framework (FIRO-AF). Step 1 is to identify reservoir design elements and operational criteria used in managing the reservoir. Steps 2 and 3 include a systematic assessment of Quantitative Precipitation Forecast (QPF) followed by streamflow forecasts that address the key design elements and operational criteria. Step 3 refers to the Preliminary Viability Assessment (PVA) and proving positive, moving on to the Full Viability Assessment (FVA). The red box denotes the steps covered by this paper.

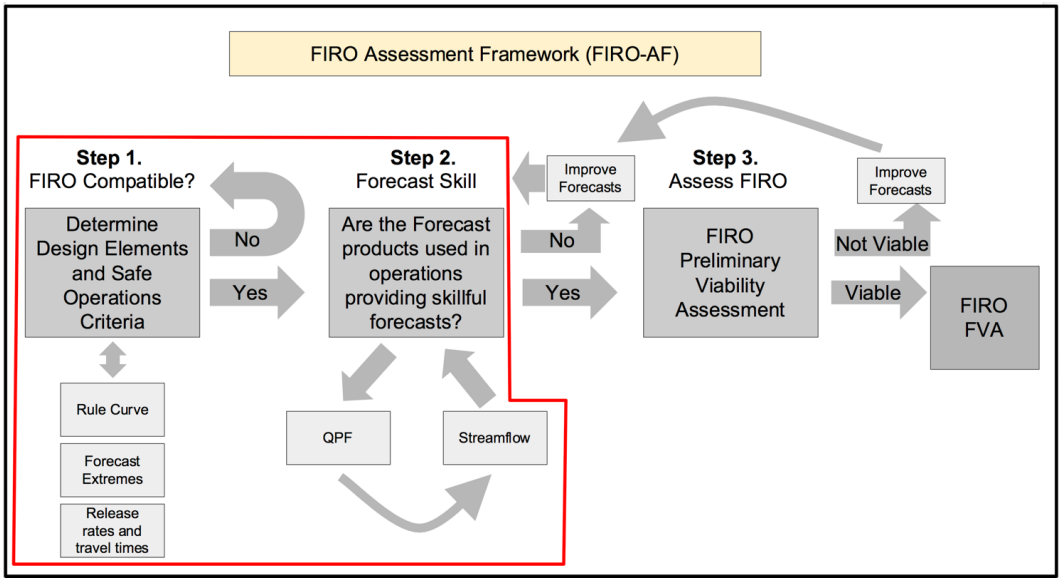

Figure 3. Lake Mendocino operational criteria (left) and storage and release framework (i.e. "rule curve", right) from the Coyote Valley Dam and Lake Mendocino Russian River, California Water Control Manual (WCM) (1959, updated 1986). The various color shadings indicate the storage levels and elevation criteria that define (left) the agency in charge of operations and (right) acceptable flood release rates based on the time of year. The maximum release rates are listed for schedules 1-3 in the right figure. *Figures adapted from Sonoma County Water Agency.*

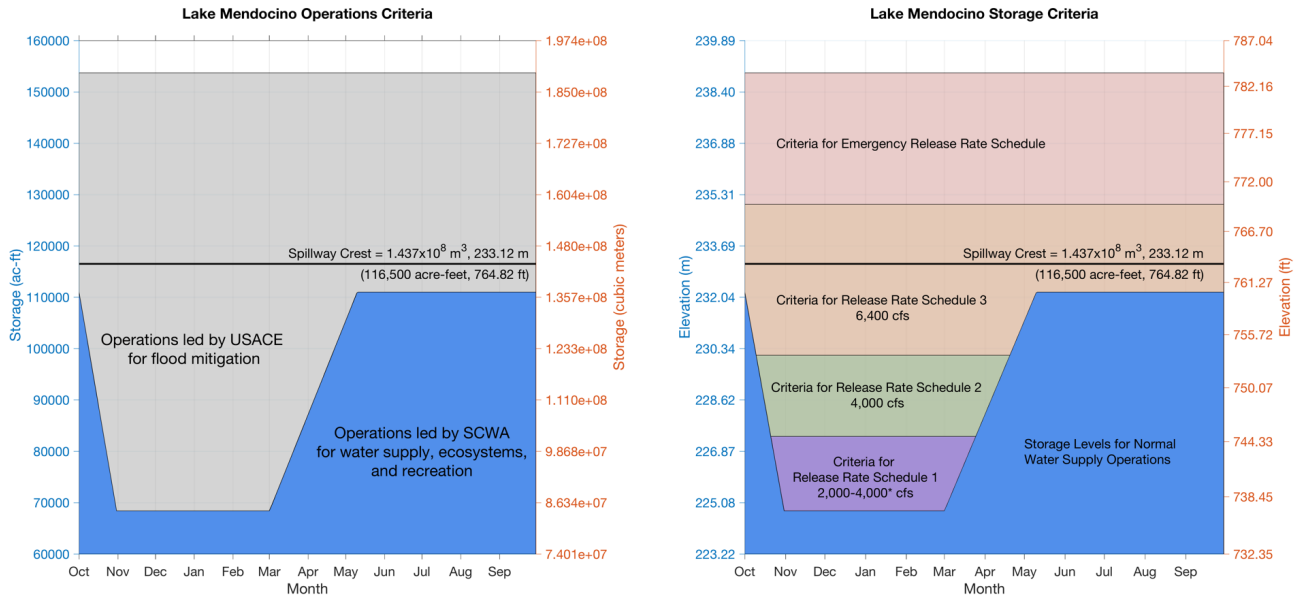

3 Coyote Valley Dam Operating Specifications

As noted in Figure 2, the first step in the FIRO Assessment Process is to determine if the reservoir design and operating criteria will allow for an effective implementation of FIRO. Figure 3 shows the operational and storage criteria as a function of the time of year. The rule curve is defined as the maximum allowable storage for flood control and mitigation. Water storage below the rule curve is considered conservation storage that serves multiple purposes, including water supply. Water storage above the elevation of the rule curve is considered flood storage for mitigating downstream flood impacts. The term "top of conservation" is often used to describe the elevation and storage that divides the conservation storage from the flood storage for a specific date of the year. During the wettest months, November to March for Lake Mendocino, the reservoir reserves space (i.e. flood pool) to store heavy runoff and protect downstream areas from flooding. As spring approaches, the rule curve increases to allow for a greater water supply pool for the dry summer months. This improve availability for municipal needs, agriculture, ecosystems, and recreation. The USACE operates the reservoir during northern California's rainy season for flood protection when reservoir storage levels are above the "conservation pool," while SCWA operates the reservoir while storage levels are below the flood pool (i.e., within the conservation pool).

The maximum water supply pool for Lake Mendocino is 137×10^6 m^3 (111,000 ac-ft). However, as noted above, during northern California's wettest months, the water supply pool is reduced to 84×10^6 m^3 (68,400 ac-ft) to allow for additional flood control capacity. The emergency spillway crest is at 144×10^6 m^3 (116,500 ac-ft) (which provides an additional flood space of 6.8×10^6 m^3 [5,500 ac-ft]). Thus, the total flood pool during mid-winter is 59×10^6 m^3. (48,100 ac-ft). When reservoir storage exceeds 84×10^6 m^3 (68,400 ac-ft), the water is evacuated as quickly as downstream limits and controls will allow. The allowances are defined in Table 1 with defined flood release rates given the level of encroachment into the flood pool. These release rates (as well as rates acceptable for ramping releases up or down) are critical in that they determine how quickly water can be evacuated safely to re-establish the flood control pool and how long the release flood wave may take to pass downstream locations. Quicker evacuations of the flood pool water can also mean less dependency on

forecast lead-time accuracy. For Lake Mendocino, maximum releases are restricted to 7 $m^3 s^{-1}$ (250 cfs) if downstream flooding is anticipated. Outflows from Lake Mendocino are reduced (following defined ramping down rates) if heavy rain is expected within the next 24-hrs or high flows (70.8 $m^3 s^{-1}$ [2500 cfs hr^{-1}]) are observed along the West Fork of the Russian near Ukiah as these factors may indicate potential downstream flooding.

Figure 4 is an example time series of current procedures for operating the reservoir and the precipitation, inflows, and reservoir storage from 1 October 2011 to 28 February 2014. It shows the reservoir water had to be released as required by the WCM (with the resulting drop in storage shown) during heavy rainfall events in early and late December of 2012. Little rain fell after those events in California and marked the beginning of the four-year drought. The maximum volume of water stored in the conservation pool is strictly defined by the time of year and is not affected by short-term weather or available inflow forecasts. Some rule curves at other reservoirs provide for the top of conservation to shift slightly up or down based on the "wetness" of the watershed. When runoff events push the storage above the top of conservation, reservoir operators must release the excess water as quickly as possible to maintain the flood control capacity. This event demonstrates the potential for FIRO to allow to modifications in the water storage retention based on a given short to medium range forecast.

Figure 4. Time series of Lake Mendocino storage (m^3, solid blue) and accumulated precipitation (mm, green) at Ukiah, CA (8km SSW of Coyote Valley Dam) from October 2011 to mid-February 2014. The normal operation storage levels (e.g. Rule Curve, red dotted line, m^3) are given for reference. Heavy rains (as indicated by the jumps in the cumulative rainfall) brought on by moderate to strong atmospheric rivers produced high inflows (cfs, black line) to Lake Mendocino in December 2012. Adapted from original image by Jay Jasperse, Sonoma County Water Agency.

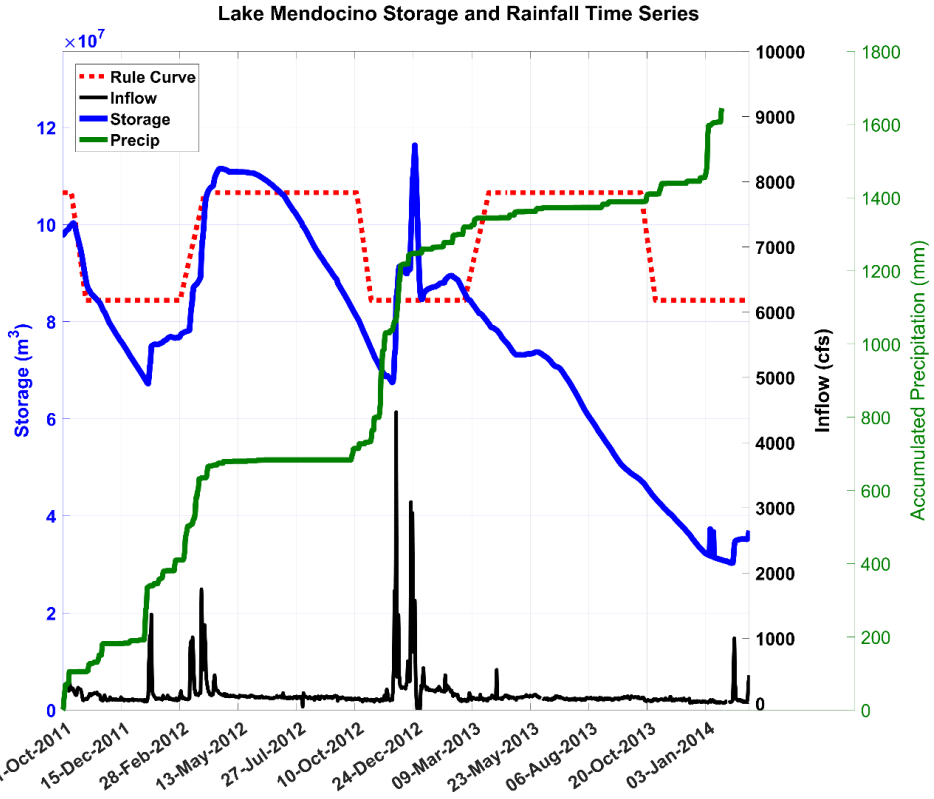

Table 1. Lake Mendocino ramping rates per USACE and National Marine Fisheries Service (NMFS).

		Hourly		Daily
Period	Release	IROC[1]	DROC[2]	DROC[2]
	(cfs)	(cfs hour^{-1})	(cfs hour^{-1})	(cfs day^{-1})
March 15 to May 15	>0 & ≤250	1,000	25	50
May 16 to March 14	>0 & ≤250	1,000	25	-
All Year	>250 & ≤1,000	1,000	100	-
All Year	>1,000 & ≤2,500	2,000	100	-
All Year	>2,500	2,000	250	-

4 Lake Mendocino Flood Wave Travel Times and Minimum Lead-time Forecast Requirements

This section covers specific forecast and lead-time requirements as established by the current Lake Mendocino WCM as well as the Preliminary Viability Assessment (PVA) developed for Lake Mendocino for FIRO (Forecast Informed Reservoir Operations Steering Committee, 2017). The lead-time analysis specifically is geared towards addressing the ability to store the target of an additional $1.34x10^7$ m^3 (10,000 ac-ft) of water in the current flood pool. The storage requirement led to the assessment of the rainfall required (approximately 50.8 mm [2 inches] 24 hr^{-1}) to produce daily inflows of $6.17x10^6$ m^3 (2500 cfs) per day (i.e. 5000 ac-ft), and how long it would take for the pre-release of $6.17x10^6$ m^3 (5,000 ac-ft) to pass by the most vulnerable locations downstream (see Figure 1 left for specific site locations). The USACE has stated that the potential for implementing FIRO at a given reservoir is the time necessary to release the additional stored water in the existing flood pool and return the reservoir to its original design operation (e.g. rule curve) (Forbis, personnel communication).

Determining Travel Times of Releases from Coyote Valley Dam to Downstream Locations: Setting Forecast Lead-Time Requirement

The WCM defines certain criteria that control the releases from CVD during flood operations. These criteria may restrict outflows during high water downstream of CVD, especially as observed at the United States Geological Survey (USGS) stream gage near Hopland (Station Number 11462500). When flows at Hopland are at or above 226.5 m^3 s^{-1} (8000 cfs), releases from CVD cannot exceed 7.08 m^3 s^{-1} (250 cfs). Because of this restriction, under a FIRO scenario, pre-releases of water from the reservoir would be desirable if the reservoir is expected to reach critical levels (e.g. approaching spillway elevations when a series of extreme rainfall events such as atmospheric rivers are expected). To minimize downstream impacts from possible high releases from CVD, it is necessary to understand the travel time of the release pulse downstream. Thus, within the WCM for CVD, flood release wave travel times from CVD to various key gage locations downstream including the last major city, Guerneville, were computed using various release volumes. These provide

a range of travel times and thus potential required lead-times for pre-releases in anticipation of a major AR making land-fall under a FIRO scenario. The travel times at key gauge locations along the Russian River are summarized in Table 2 as well as minimum, maximum, and median flow values for each location. It is difficult to assess the diffusion rates or amplification of a specific flood wave release rate as it travels downstream using observations alone. Instead, using the median flows as guidance for pre-release conditions, the anticipated time for a flood wave to travel past Guerneville would be 2.81 days once releases were stopped. The difference between the minimum and maximum discharges at each site indicates a large spread in streamflow conditions. Higher streamflow rates would decrease the travel time while lower discharge rates would increase travel times. However, the lowest discharge rates are usually indicative of extremely dry conditions in which the runoff efficiency is low (i.e. water storage in soils and/or stream losses). If the required release of 1.34×10^7 m^3 (10,000 ac-ft) of water takes 2 days, then the compounding effect of release plus travel means a minimum forecast lead time between 4 and 5 days. Release rates up to 113.25 $m^3 s^{-1}$ (4,000 cfs) are authorized within flood control level 1 (see Figure 2) and thus this could reduce the lead-time to just over 3 days. Barring unforeseen release restrictions, these results support a 3 to 5-day forecast lead-time requirement of a significant precipitation event.

Table 2. Approximate flood wave travel times (hours) per discharge rate (cfs, bottom row) from the WCM, median, maximum, and minimum discharges (cfs), and distances (mi/km) at and between key locations along the Russian River watershed. The gage locations along the Russian downstream of CVD are plotted in Figure 1. The minimum, maximum, and median discharge rates at the endpoint location are calculated from USGS records between 2000-2018.

Travel Time Location	Travel Times (hours) per discharge rate									End Point Median Discharge (cfs)	End Point Maximum Discharge (cfs)	End Point Minimum Discharge (cfs)	Distance between gauges in mi (km)
Forks to Hopland	11	9	7.5	6.5	6	6	5.5	5	4.5	329	35,600	27	14 (22.54)
Hopland to Cloverdale	12.5	9	7	5.5	5	4.5	4	3	2.5	452	50,700	23.9	16 (25.75)
Cloverdale to Healdsburg	18.5	13	10.5	9.5	8.5	8	7.5	6.5	6	889	58,900	100	28 (45.06)
Healdsburg to Guerneville	43	31	26	21	19	18	16.5	14	13	1080	86,000	68.7	16 (25.75)
Discharge Rates (cfs)	400	1,000	2,000	4,000	6,000	8,000	10,000	20,000	40,000				

5 Assessing the Baseline Skill of Forecast Products and Observations for Lake Mendocino

The engineers in charge of operating and managing water storage use forecasting information to make informed decisions concerning reservoir release schedules and storage targets based on QPF and hydrological streamflow forecasts. These forecasts are produced by the California-Nevada River Forecast Center (CNRFC), (Marchia V. Bond, Personal Communication), which provides 120-hr QPF, reservoir inflow, and streamflow forecasts for major control points located within the Russian River watershed. The focus of this paper only discusses NWS products produced for Lake Mendocino. The QPF and inflow forecasts are described next. These forecasts can provide situational awareness for upcoming extreme events as well as to inform operators that little significant rainfall or inflow is expected.

Operational Reservoir Products: Quantitative Precipitation Forecasts

The NWS issues 6-hr Mean Areal Precipitation (MAP) QPF forecasts beginning at 1200 UTC and extending out 5 days. Forecasts are updated at least twice per day in the rainy season and up to four times per day during flood events. Only the first daily issuance of the QPF was used for this analysis. CNRFC Hydrometeorological Analysis and Support (HAS) meteorologist can choose from a wide range of inputs to begin their forecast process, including short- and medium-range model forecasts, the National Center for Environmental Prediction (NCEP) Weather Prediction Center (WPC) forecast, and National Weather Service (NWS) Weather Forecast Office (WFO) forecasts. The HAS meteorologist reviews the RFC regional gridded-point values for a specified number of sites throughout the RFC region and, when appropriate, modifies these points to the local terrain, regional climate, and sensitivity of hydrologic models to precipitation. From 2010 forward, the HAS unit utilizes the NWS Graphical Forecast Editor (GFE) software (Glahn et al. 2003) to perform these operations. Prior to 2010 the HAS unit used a simplified tool known as Specify (Mountain Mapper developed by the Colorado Basin River Forecast Center [Henkel and Peterson 1996]). The HAS forecaster provides a QPF forecast for almost all of California, Nevada, and extreme southern Oregon. The area encompassing Lake Mendocino is thus a very

small portion of the forecast area. The adjusted QPF point values are then input into the Parameter-elevation Regressions on Independent Slopes Model (PRISM; Daly et al. 1994)-based Mountain Mapper software to interpolate the QPF data points to a 4-km Hydrologic Rainfall Analysis Project (HRAP) grid. Between gauge locations, a double linear interpolation technique is applied to a triangulated irregular network to vary the bias for each grid (Daly et al. 1994). The result is a unique bias for each 4 km × 4 km grid. Using these products, it is possible to capture localized precipitation patterns that are often missed in the coarser national product grids.

Operational Reservoir Products: Inflow Forecasts

Like the QPF data, 5-day lead time inflow forecasts are issued by the NWS twice per day during the rainy season (October through April), once per day in the dry season (May through September), and up to every six hours during flood events. These forecasts are deterministic and are produced by the Community Hydrologic Prediction System (CHPS) (Werner et al. 2013). CHPS was developed by the NWS in collaboration with Deltares (formerly Delft Hydraulics) of the Netherlands. For this analysis, the forecast data at every 6 hours, representing instantaneous increments beginning at 18Z (10am PST) for each day and includes 20 forecast ordinates (4 forecasts per day for 5 days), are used. Observed values were also provided for each forecast ordinate. It should be noted that from 2000-2010, the long range CNRFC 4 to 5-day QPF were generated from the Rhea orographic model (Rhea 1996). Trends in forecast skill over time and/or methodology are not assessed in this report, but rather the skill of a CNRFC forecast as it would have been received by a dam operator is investigated herein.

Verification Data and Metrics

The Quantitative Precipitation Estimation (QPE) data used for verification in this study are 6-hour accumulated precipitation amounts produced by the CNRFC on a 4-km *HRAP* grid (Stage IV, Nelson et al. 2016). These 6-hr amounts are summed to produce 24-hour, and 72-hr and 120-hr total MAP values for the Lake Mendocino watershed. Unlike other parts of the CONUS, where radar data are combined with rain gage data, the CNRFC only uses rain gage observations.

The measures selected for assessing forecast accuracy and skill include:

- Root Mean Square Error (RMSE), which is calculated as the square root of the average of the squares of the errors (the difference between the observed values and the forecasted value squared) and the expected error (bias) is calculated as the difference between the forecast value and the average observed value.

- The Coefficient of Determination (R^2), which represents a measure of how well the forecasts are replicated by the model when compared to observations.

- Contingency table-based Hits, False Alarms, and Misses (Mason 2003). When a forecast has both an observed and a predicted event, a hit (H) occurs. When a forecast has a predicted event that is not observed, a false alarm (FA) occurs. Lastly, when a forecast has an observed event that is not predicted, a miss (M) occurs.

- The Probability of Detection (POD), which represents the ratio of the number of correct forecasts (H) to the number of observed events (H+M). Ranges from 0 to 1. A perfect POD is 1.

- The False Alarm Rate (FAR), or the ratio of the number of false alarms (FA) to the number of forecasts made (H+FA). Ranges from 0 to 1. A perfect FAR is 0.

- The Critical Success Index (Threat Score), which is calculated as the ratio of the correct forecasts (H) to all events either forecasted or observed (H+M+FA). Ranges from 0 to 1. A perfect CSI is 1.

The POD, FAR, and CSI scores are used to assess 25.4 mm (1 inch) and 50.8 mm (2 inch) 24 hr^{-1} forecasts and are calculated using a simple 2x2 contingency table comparing the forecast at or above a given threshold to the observed amount (Table 3). The POD is sensitive to hits and thus makes it a good measure for rare events, but it can be artificially improved by over-forecasting to increase the number of hits. The FAR is sensitive to false alarms but ignores misses. Like the POD, the FAR is very sensitive to the climatological frequency of the events (number of hits), and therefore, should be used in conjunction with the POD for optimal forecast performance feedback. The CSI is sensitive to hits and it penalizes for both misses and over-forecasting (false alarms). However, rare events are not represented well with the CSI because this score depends on the

climatological frequency of events thus resulting in lower scores for rarer events (Mason 1989). It is therefore useful to look at all three of these measures to interpret the quality of the forecast.

Table 3. Contingency table of the four possible outcomes for categorical forecasts of a binary (yes/no) event.

Events	Observed (O)	Not observed
Forecast	Hit (H)	False alarm (FA)
Not Forecast	Miss (M)	Correct rejection

CNRFC QPF and Inflow Verification for Lake Mendocino Watershed

In this section, a verification of the CNRFC MAP (herein QPF) over the watershed above Lake Mendocino from 2000-2017 and inflow forecasts for the period 2005-2017 is presented. While the 6-hour forecasts of QPF (inflow) are important for timing of peak precipitation (inflow), the ability to predict the exact timing of intense precipitation using multi-day lead times is quite challenging (e.g. Demargne et al. 2014). The correlation of 6-hourly QPF to observations drops below 0.5 using lead times greater than 2.5 days. Instead, the 6-hourly forecasts for QPF and inflow are aggregated into 24-hour totals to match WCM manual stipulations (i.e. 25.4 mm [1 inch] 24 hr^{-1}), and 72, and 120-hour totals because total inflows over 1, 3, and 5 days are what would trigger pre-releases under FIRO. The mean non-zero 24-hour total precipitation over the watershed is 11.53 mm (0.454 inches) with a standard deviation of 14.73 mm (0.58 inches).

Figure 5 shows the 24-hr total QPF and inflow RMSE and the coefficient of determination (R^2) as a function of lead time between 0 to 5 days. QPF R^2 exceeds 0.5 using information up to a 4-day lead time, indicating a strong correlation of 24-hr forecasts to observations. In fact, the 120-hr total QPF explains 88% of the total variance in observed MAP with an RMSE of 12.5 mm (0.58 inches) (Table 4). A small wet bias (0.5 mm [0.02 inch]) is found for days 1-3 and a slight dry bias (0.254 mm [-.01 inch) for days 3 through 5. The 24-hr total inflow forecasts statistics as a function of lead time are plotted in Figure 5 (bottom) and summarized along with 72-hr and 120-hr totals in Table 5. Results show a gradual decrease in R^2 with a forecast day 1 value of 0.9 but exceeding 0.5 for all lead times. The inflow

RMSE is between $5x10^5$ m^3 (415.2 ac-ft) using 1-day lead time forecasts and $8x10^5$ m^3 (663.5 ac-ft) using 5 day lead time forecasts (62% increase). This represents 8.3-13% of maximum daily release allowances from the lake. Forecasts on shorter lead times (days 1-2) are slightly overestimated while forecasts from longer lead times (3 to 5 days) exhibit a slight underestimation of inflow. 72-hr and 120-hr forecast volumes show similar but strong positive correlations to the observations with 72-hr R^2 exceeding 0.5 at 3 through 5-day lead times. The 72-hr RMSE increases roughly 22% with lead time with a negative bias for the 1-day forecast lead-time and a positive bias for the 2 and 3-day forecast lead-time. The 120-hr forecasts of inflow show an overall underestimation.

The statistics in Table 4 and Table 5 are indicative of the forecasts made during the cool-season and reflect both dry and wet periods. However, 90% of the days during the cool season exhibit less than 25.4 mm (1 inch) of rainfall over the watershed. Thus, a persistence forecast less than 25.4 mm (1 inch) MAP would be right 90% of the time. The CNRFC MAP forecasts were also analyzed for periods of rainfall greater than 25.4 mm (1 inch) 24 hr^{-1} and the potential misses, false alarms, and hits using this threshold. The skill scores of QPF > 25.4 mm (1 inch) 24 hr^{-1} as a function of lead times is given in Figure 6. For QPF forecasts > 25.4 mm (1 inch) 24 hr^1, the POD exceeds the FAR up to a 3-day lead time. This means that the minimum forecast skill of a significant precipitation event (enough to consider pre-releases) is just within the spectrum of the FIRO forecast requirements (3 to 5 days). The actual impacts of the releases will depend on the storage levels at the time and downstream water levels. For context, the CONUS WPC critical success index of the single cool season all-time records is also plotted for forecasting 25.4 mm (1 inch) 24 hr^{-1} (0.49 for 1 day, 0.42 for 2 days, and 0.38 for 3 days). Although there is an obvious scale difference between the CONUS and this small watershed, the CNRFC forecasts skill level is at or above the all-time WPC records out to 3-day lead time. The correlations for QPF greater than 50.8 mm (2 inches) per day (not shown) were greater than 0.5 and exceeded the WPC CONUS all-time single cool-season CSI values out to 2 days lead time.

Forecasting dry periods is valuable to a FIRO implementation because water could potentially be reserved in the flood pool until the next forecasted event with significant rainfall (greater than 25.4 mm [1 inch]). This section is presented in terms of forecast evaluations of no significant rainfall. This means that a miss is defined as the condition in which the

forecast was greater than 25.4 mm (1 inch) 24-hr^{-1} but less than 25.4 mm (1 inch) was observed. The number of hits would correspond to the condition in which forecasts accurately predicted no significant rainfall. A false alarm means the CNRFC forecasted less than 25.4 mm (1 inch) and more than 25.4 mm (1 inch) was observed. Table 6 shows the number of hits, misses and false alarms when the CNRFC forecasts were for less than 25.4 mm (1 inch) 24 hr^{-1}. Results indicate a very high hit rate for forecasting no significant rainfall (recall 90% of the cool season days observe less than 25.4 mm [1 inch] of rain) and an increasing miss and false alarm rate with lead time. Depending on the magnitude of the forecast error, a miss could mean that water might be unnecessarily pre-released for an expected significant event which does not occur. These are the cases of most concern depending on the magnitude of the error for these instances. Any large under-forecast could result in an uncontrolled release if the reservoir was deeply encroached into the flood pool. Table 7 shows the number of false alarms and the mean error when the 1, 3, or 5-day 24-hr MAP forecast was for less than 25.4 mm (1 inch) and the observed MAP was over 25.4 mm (1 inch) with the forecast error greater than 25.4 mm (1 inch). The mean error for these cases was just over 25.4 mm (1 inch). If there is a forecast of no significant rainfall in the next five days, no pre-releases would be made within a time frame to assure the release wave is past Guerneville. As lead time of a significant rainfall decreases, it would be more difficult to make pre-releases without contributing to larger flows downstream. One notable event with a 76.2 mm (3-inch) error on a day 5 forecast occurred on 25 January 2008. The observed inflow for this event was 2400 cfs per day (~ 4800 ac-ft). The day 3 forecast was just over 25.4 mm (1 inch) but resulted in a 50.8 mm (2 inch) underestimate. Given the 3-day forecast was over for 25.4 mm (1 inch), the dam operator would be alerted to potential larger inflows but under FIRO may not pre-release enough water. Again, this would only be of real concern if the reservoir was within 6.17×10^6 m^3 (5,000 ac-ft) of spilling.

Finally, the distributions of forecasts for three ranges of observed 24-hr precipitation are compared to determine whether there is a distinct discrimination of forecasted MAP between categories of precipitation events. Figure 7 shows the distribution of the 24-hr QPF as a function of lead time separated into groups where the observed event was less 25.4 mm (1 inch), greater than 25.4 (1 inch) mm but less than 50.8 mm (2 inches), and greater than 50.8 mm (2 inches). At 4 to 5-day lead times,

the QPF of the events greater than 50.8 mm (2 inches) has significant overlap with the other two categorical event types, indicating a large uncertainty in the categorical outcome of a forecast at the 5-day length scale. The spread of the 4 to 5-day lead time forecast spans 0 to 85 mm and almost all forecasts underestimated the > 50.8 mm (2 inches) event. Both categories of rainfall greater than 25.4 mm (1 inch) exhibit a clear trend (e.g. increasing precipitation forecasts) as lead time decreases. At 2 days lead time or less, there is a greater distinction (little overlap of boxes) of forecasts of each category and a better likelihood of verification between each of the three rainfall categories. The separation of the distributions of forecasts is important in terms of making decisions based on the potential of significant rainfall. In the next section, significant rainfall are classified into extreme events based on historical return periods and explore whether there are similar forecasting tendencies of large events on longer time scales relevant for FIRO operations.

Figure 5. Coefficient of determination (R^2, solid lines) and root mean square error (RSME, dashed lines) for the CNRFC's 24-hour accumulated QPF (mm, top) and inflow forecasts (m^3, bottom). The 24-hour QPF and inflow totals are from aggregated 6-hour forecasts during the cool season (Oct – Apr) over the period of record from 2000-2017 and 2005-2017, respectively. R^2=0.5 is drawn in gray for reference.

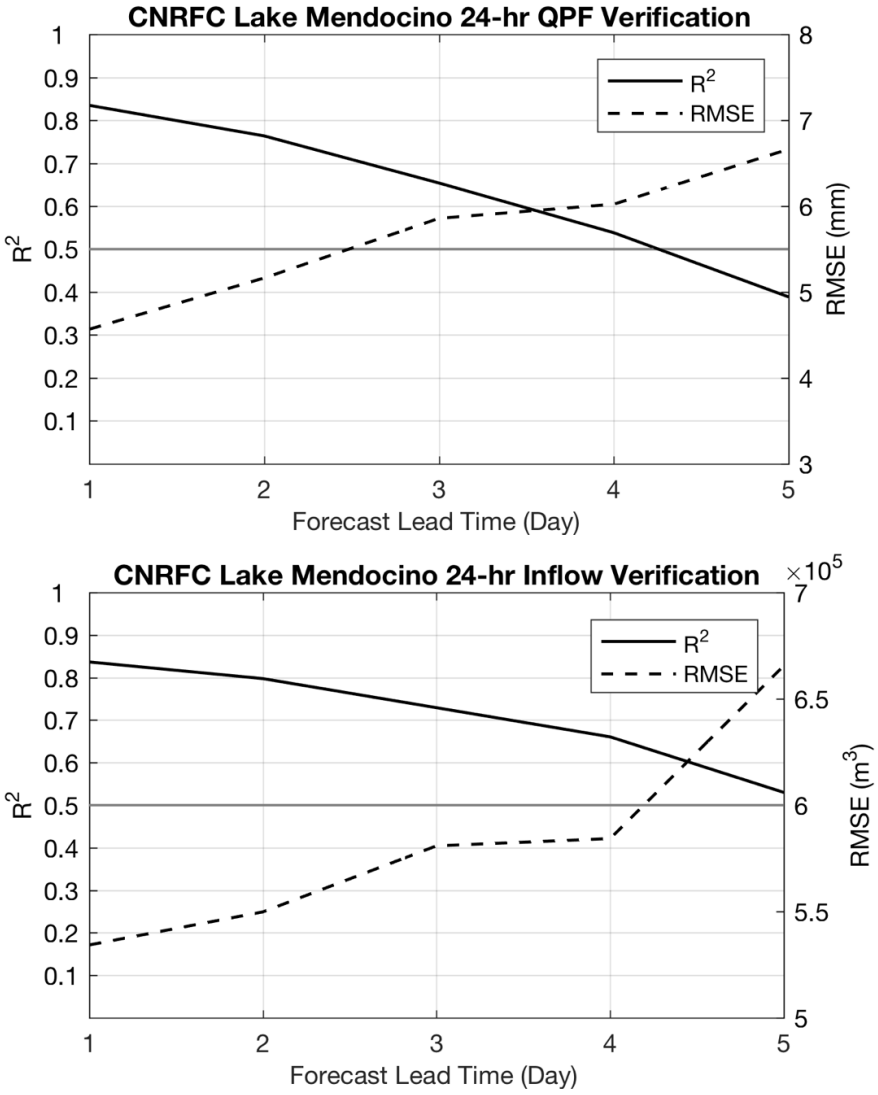

Table 4. Coefficient of Determination, RMSE, and bias for CNRFC 24-hr, 72-hour, and 120-hour accumulated QPF for Lake Mendocino watershed as a function of lead time. The QPF is calculated during the cool season between January 2000 and May 2017 was used for this comparison

	Lead Time				
Accumulation Metric	1 day	2 days	3 days	4 days	5 days
24-hr R^2	0.83	0.76	0.65	0.54	0.39
24-hr RMSE [mm (inches)]	4.57 (0.18)	5.08 (0.20)	5.84 (0.23)	6.10 (0.24)	6.60 (0.26)
24-hr bias [mm (inches)]	0.51 (0.02)	0.51 (0.02)	0.25 (0.01)	-0.25 (-0.01)	-0.51 (-0.02)
72-hr R^2			0.83	0.77	0.68
72-hr RMSE [mm (inches)]			8.13 (0.39)	9.65 (0.41)	11.17 (0.46)
72-hr bias [mm (inches)]			2.29 (0.05)	1.51 (0.02)	-0.51 (-0.02)
120-hr R^2 *					0.79
120-hr RMSE* [mm (inches)]					10.67 (0.58)
120-hr bias* [mm (inches)]					3.81 (0.03)

Table 5. Same as Table 4 for inflow forecasts for the period January 2005 to March 2017.

	Lead Time				
Accumulation Metric	1 day	2 days	3 days	4 days	5 days
24-hr R^2	0.84	0.80	0.73	0.66	0.53
24-hr RMSE [m^3 (ac-ft)]	$5.34x10^5$ (433.13)	$5.498x10^5$ (445.74)	$5.809x10^5$ (470.93)	$5.843x10^5$ (473.70)	$6.656x10^5$ (539.60)
24-hr bias [m^3 (ac-ft)]	$2.487x10^4$ (20.16)	$1.547x10^4$ (12.54)	$-1.209x10^4$ (-9.80)	$-4.380x10^4$ (-35.51)	$-4.560x10^4$ (-36.97)
72-hr R^2			0.85	0.81	0.75
72-hr RMSE [m^3 (ac-ft)]			$1.243x10^6$ (1007.86)	$1.285x10^6$ (1041.55)	$1.389x10^6$ (1125.80)
72-hr bias [m^3 (ac-ft)]			$2.716x10^4$ (22.02)	$-4.396x10^4$ (-34.83)	$-1.045x10^5$ (-84.68)
120-hr R^2 *					0.83
120-hr RMSE* [m^3 (ac-ft)]					$1.930x10^6$ 1564.723
120-hr bias* [m^3 (ac-ft)]					$-6.689x10^4$ (-54.23)

Figure 6. CNRFC Lake Mendocino 24-hr QPF skill scores of probability of detection (POD, dotted), false alarm rate (FAR, dashed), and critical success index (CSI, solid). The skill scores are computed from 6-hour QPFs during the cool season (Oct – May) from 2000 – 2017. The WPC CSI all-time-record scores over CONUS during the cool season (x's) are plotted for reference.

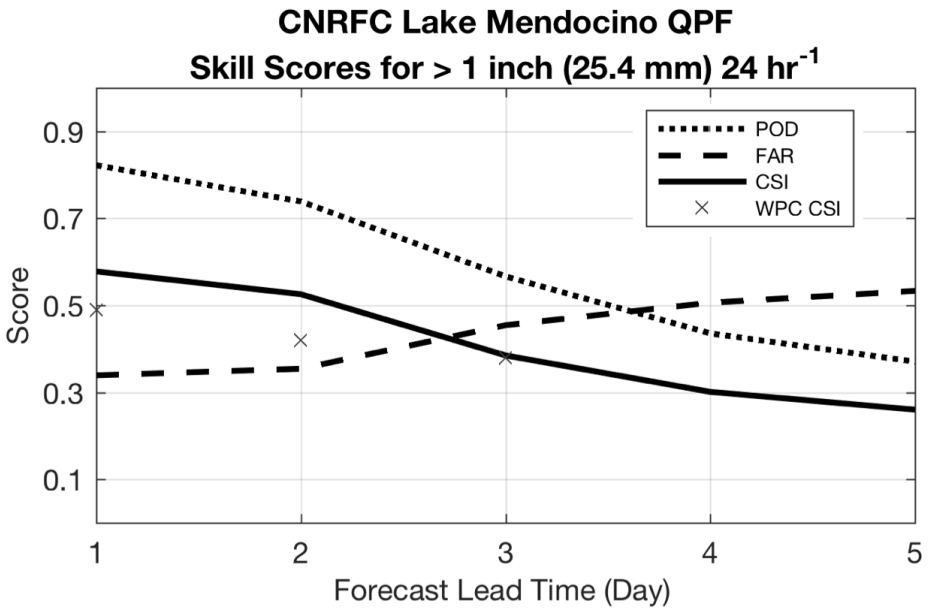

Table 6. Number of forecasts, hits, misses and false alarms when CNRFC Lake Mendocino QPF is 1 inch or less of rainfall per day (2000-2017 data).

Lead Time	# Forecasts	Hits	Misses	False Alarm
Day 1	3859	3606	75	32
Day 2	3859	3608	73	46
Day 3	3859	3595	86	78
Day 4	3859	3597	84	102
Day 5	3859	3599	82	115

Table 7. Number of false alarms per specified forecast lead-time along with the mean and maximum error when the CNRFC Lake Mendocino QPF was below 1 inch (25 mm) per day, the observed rainfall was over 1 inch, and the forecast error exceeds 1 inch. The dates and the magnitude of the top three forecast errors are also listed.

Forecast Lead-time Days	# of Misses	Mean Error (mm)	Maximum Error (mm)	Dates of top 3 misses and error mm (inches)
Day 5	55	-37.4 (-1.47 in)	76.5 (3.01 in)	01/25/2008 -76.5 (-3.01) 12/21/2015 -70.0 (-2.76) 02/16/2004 -66.3 (-2.61)
Day 3	21	-33 (-1.3 in)	49 (1.93 in)	02/06/2017 -49.0 (-1.93) 11/21/2001 -45.5 (-1.79) 12/09/2016 -42.9 (-1.69)
Day 1	3	-27.7 (-1.09 in)	30 (1.18 in)	02/12/2000 -30.0 (-1.18) 04/16/2000 -28.0 (-1.10) 02/19/2002 -27.4 (-1.08)

Figure 7. 24-hr QPF distributions as a function of lead time (days) separated by 24-hr QPE (i.e. Obs) greater than 0.1 inches 24 hours^{-1} but less than 1 inch per day (blue boxes), greater than 1 inch per day (green boxes) and greater than 2 inches per day (red boxes). The box in the middle represents the median, the edges of the box represents the 25th and 75th percentiles, and the markers outside the whiskers represent the outliers of the 95th percentile. The gray lines are drawn at 25.4 mm (1 inch) and 50.8 mm (2 inches) for reference. The green and red boxes were drawn offset from the lead time for clarity.

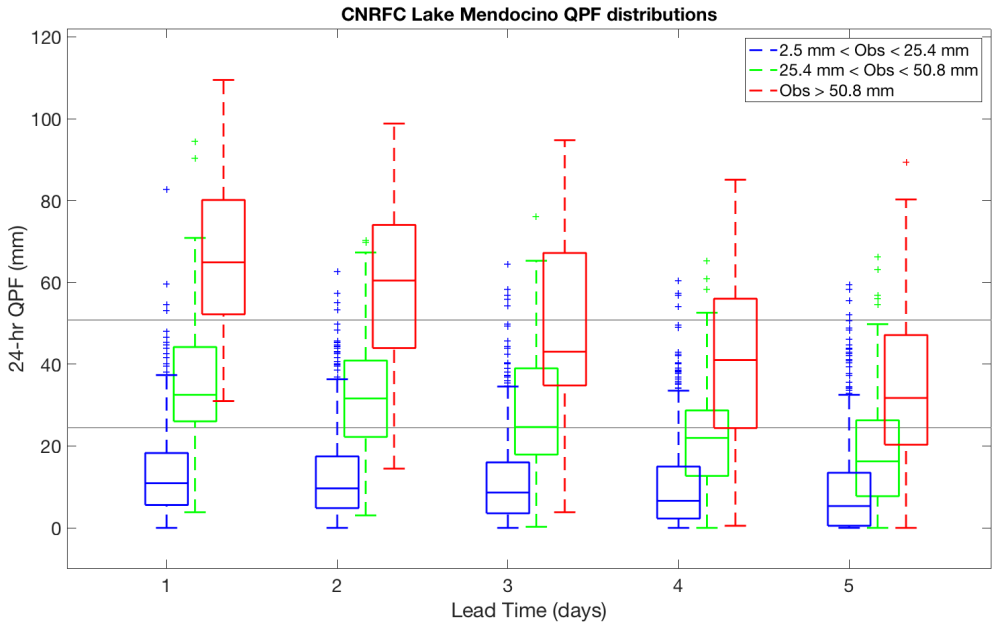

QPF and Inflow Scale Extreme Event Skill

This section focuses on the distribution of extreme QPF and inflow forecasts for Lake Mendocino and their forecast errors on timescales relevant for FIRO operations. The historical frequency, or return rates, of watershed precipitation over and inflow rates into Lake Mendocino will be used to classify the upper bounds of the distribution of QPF and inflows. Quantifying the forecast error tendencies or biases of these "extreme" events may provide insight into underlying precipitation predictability on watershed scales and the resulting hydrologic impacts.

Figure 8 shows the calculated return periods of 24-hr, 72-hr, and 120-hr mean areal precipitation yearly maximum time series observations from 1980-2017 and full natural flows from 1959-2011 at Lake Mendocino. Note, the full natural flows were used in place of inflows to better approximate the climatology of runoff without the influence of dam releases, specifically from a reservoir along the Eel River that is diverted through a tunnel to the East Fork of the Russian. The return periods are defined as:

$$Rp = \left(\frac{(2n-1)}{2y}\right)^{-1} \qquad (1)$$

where y is the total number of events in the time series and n is the rank (from 1 to y) of each event in the time series. When the probability of a large event is small, the return period is large. A 2-year return period was chosen as a threshold for precipitation and inflow extrema as it corresponds to the upper 99th percentile of observations made during our study period of record and upper 50% of the maximum yearly ranked events. The sample size of extreme events significantly decreases with increasing return periods. A 2-yr return period was also chosen to provide enough data samples during the analysis period. Using a logarithmic function fitted to the return period trend of precipitation and inflow, the 2-year return period 24-hr, 72-hr, and 120-hr precipitation accumulations are 64.49 mm (2.539 inches), 120.24 mm (4.734 inches), and 152.273 mm (5.995 inches), respectively. The 24-hr 2-year return period falls almost half way between the 1 and 0.1% exceedance values Sukovich et al. (2014) found for the entire CNRFC forecast domain using 2000-2011 observed rainfall. The corresponding 2-yr return periods of 24-hr, 72-hr, and 120-hr

full natural flows are $8.327x10^6$ m^3 (6751.6 ac-ft), $1.850x10^7$ m^3 (14,995 ac-ft), and $2.434x10^7$ m^3 (19,764 ac-ft), respectively.

First, the forecast errors of extreme precipitation and inflow were evaluated against the forecast magnitude to identify potential patterns that could be leveraged in future operations (Figure 9). This analysis only considers events with forecasts that were greater than or equal to a 2-year return period (Figure 8) at 72-hr and 120-hr lead times (in order to stay consistent with FIRO time scales). Each forecast was treated independently; thus, there are cases in which multiple 120-hr forecasts exist for the same meteorological event, depending on its duration. For these extreme events (forecasted and observed), there is a tendency to under-forecast the largest observed precipitation and inflow events according to the observed 120-hr totals and over-forecast those events whose observed magnitude has less than a 2-year return period. While the 120-hr totals are an aggregation of many forecasts over time, they are still subject to timing errors at the beginning and ends of the aggregation time frame. The combination of timing and amplitude errors may explain the smaller R^2 value.

The 47 120-hr forecasts that are plotted in Figure 9 are analyzed to examine the contribution of the individual days that make up the 120-hr forecast to the overall 5-day error. There is a slight tendency for the 3 to 5 day forecasts to contribute more to the overall error when the 120-hr forecast error is greater than 25.4 mm (1 inch). There is higher variance in the forecast errors for days 3 to 5 as well. However, the largest single errors for the day 1 to 5 forecast occurred on both day 5 (88.9 mm [-3.5 inch] error) and day 1 (67.82 mm [+2.67 inch] error). The mean of the daily errors (bias) is consistent with the overall biases noted in Table 4. That is, there is a negative bias for days 3 to 5 and a positive bias for days 1 to 2.

Each of the events plotted in Figure 9 were classified as ARs using the criteria developed by Rutz et al. (2014) using the Modern-Era Retrospective analysis for Research and Applications, Version 2 (MERRA2) (Gelaro et al. 2017). Large errors can generate from displaced AR landfall locations (and resulting precipitation) by as much as 200 km at 1-day lead times to 600 km at 5-day lead times (Wick et. al 2013). These are much larger scales than the size of the Lake Mendocino watershed. The linear relationship between forecasts of precipitation and inflow and

their associated forecast errors are weak (small R^2) and may be indicative of the difficulty to capture the extremes in a forecast (larger number of false alarms and misses). The correlations do not increase with increasing sample size (e.g. smaller return period) (not shown).

Figure 10 shows the comparison of contemporaneous 72-hr and 120-hr QPF and inflow errors for forecasted or observed inflow greater than a 2-year return period. The strong correlation between QPF errors and inflow errors is not surprising as the inflow forecast are heavily dependent on the rainfall forecasts either through processes related to infiltration-excess in times of intense precipitation rates and/or saturated soils that support runoff generation. However, it can be used to quantitatively estimate the potential impacts of large event precipitation prediction uncertainty on inflow using a regression as guidance. This is an economical approach to estimate of inflow change due to forecast uncertainty without having to run a full hydrologic model or use broad assumptions based on the unit hydrograph. The 120-hr errors show a positive inflow bias with respect to the precipitation errors for extreme events. Errors of 25.4 mm (1 inch) from a 120-hr QPF forecast translates to an error of 7.95×10^6 m^3 (6443 ac-ft) when accounting for the positive bias in inflow error at Lake Mendocino. Inflow volume of this magnitude is meaningful as it corresponds to the upper 88th percentile of all cool-season 120-hr inflows into Lake Mendocino. Underestimated precipitation errors of 25.4 mm (1 inch) corresponds to approximately 2.20×10^6 m^3 (1784 ac-ft). The positive bias in inflow errors means that more water could be pre-released in an over-forecast scenario than gained in an under-forecast scenario. Decisions based on forecasted precipitation uncertainty, while out of the scope of this paper, could potentially leverage this uncertainty when accounting for soil saturation and flood pool storage. Estimations of inflow error dependence on QPF errors could also aid targeted watershed-scale hydrologic studies in the West in which rainfall is the major factor of uncertainty in inflow and streamflow modeling (as compared to parameterizations [e.g. Butts et al. 2004)]. Radar coverage in the West is hindered in areas of mountainous terrain and decisions on the appropriate precipitation forcing from observations (including understanding its errors on watershed scales) is a recommended key step in any hydrological study (Cuo et al. 2011).

Figure 8. Return periods for 24-hr (purple dots), 72-hr (blue diamonds), and 120-hr (red squares) MAP (left) and inflow (right) over the Lake Mendocino watershed. A logarithmic function (colored lines) is fitted to represent the relationship of return period frequency to the magnitude of precipitation and inflow, respectively

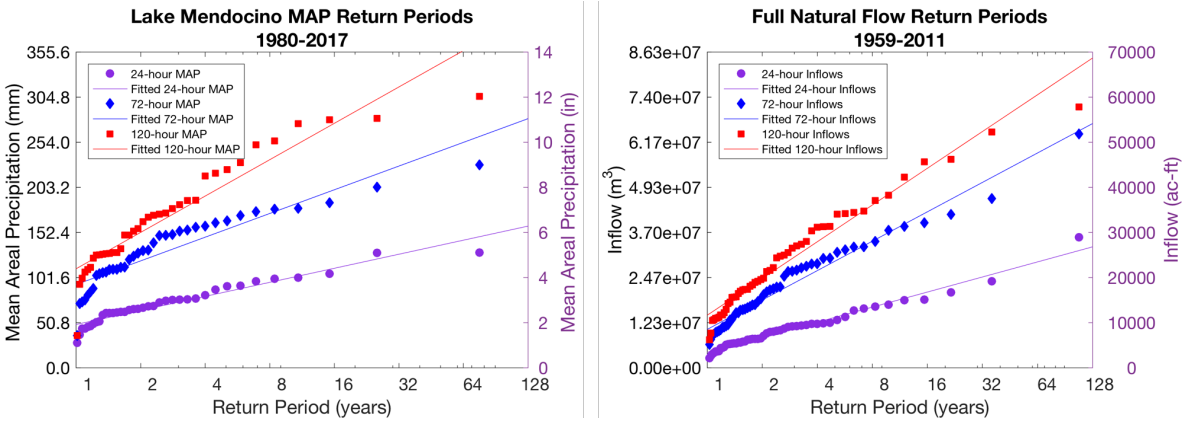

Figure 9. Comparison of 120-hr forecast errors of Lake Mendocino (left) MAP (mm) and (right) forecasted inflow (m^3) to CNRFC 120-hr (left) QPE (mm) and (right) observed inflows (m^3). The black circles represent the errors when the forecast exceeded the 2-year return period threshold and the blue diamonds represent when the observations were greater than a 2-year return period event. The coefficient of determination fitted to both sets of data is listed in the bottom left corner of each panel.

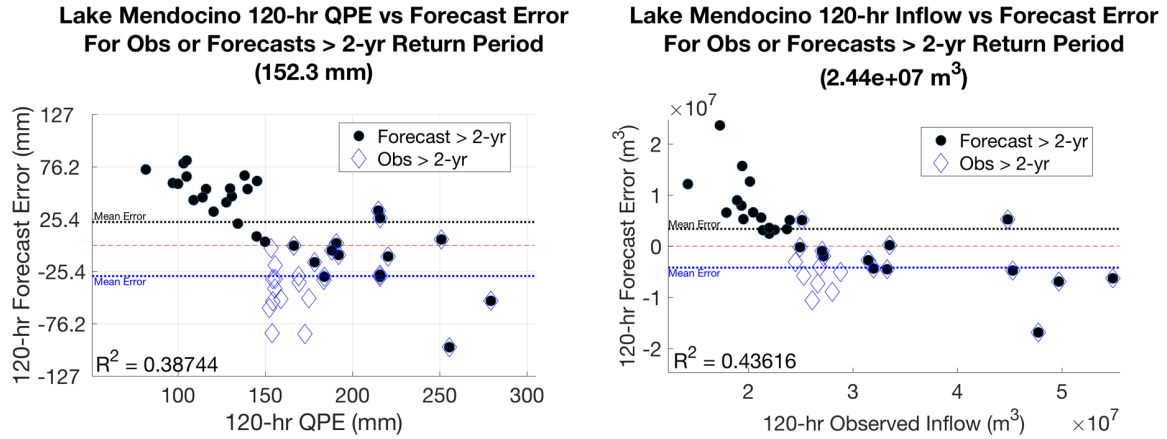

Figure 10. Regressions of 72-hour (top) and 120-hour (bottom) forecasted inflow errors to their respective QPF errors using inflow values greater than a 2-year return period inflow. The 3 to 5 day forecasts errors (i.e. using 3 day lead time forecasts) are plotted for the 72-hr totals. The best fit line is drawn in dark blue and the 90% predictive bounds of the best fit are drawn in light blue. Upper left inset: coefficient of determination, equation describing 1-degree polynomial best fit with the general form F(x) = ax+b where a is in units of mm and b is in units of m^3.

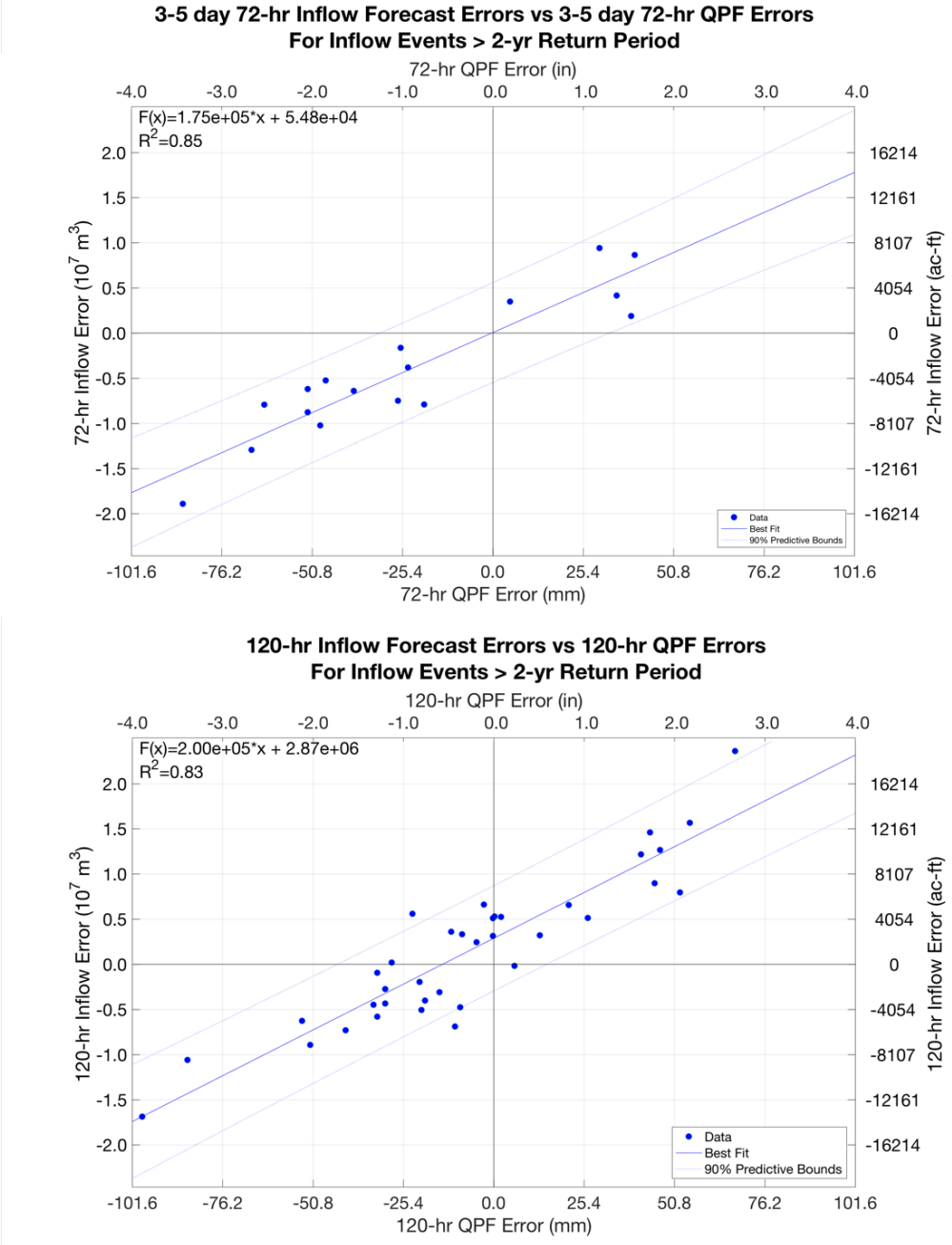

6 Summary and Discussion

This paper identifies and analyzes the Lake Mendocino reservoir design elements, operating criteria, and forecasts of precipitation and inflow over approximately the last two decades as part of a FIRO assessment framework defined herein. The FIRO assessment framework describes potential steps to assess the viability of FIRO at any given reservoir. This report addresses the first two of the three steps by analyzing rainfall forecasts for the watershed, subsequent inflow forecasts, and operating requirements based on the WCM for Coyote Valley Dam. The CNRFC forecast skill is evaluated on time scales based on those requirements.

The operational criteria in the WCM specifies how the reservoir is to be operated especially during periods when the reservoir is encroached into the defined flood space (i.e. current storage in the flood pool, water release and ramping rates, and river flows downstream). The time in which a FIRO-driven pre-release flood flow makes it past vulnerable locations along the river is critical to eliminating any potential for aggravating downstream flooding. For typical (median) inflows of the Russian River, a pre-release flood wave of 1.23×10^7 m^3 (10,000 ac-ft) could take up to 5 days to travel past vulnerable communities downstream prior to precipitation runoff. Higher flows in the river would correspond to shorter travel times (e.g. 3 days assuming a minimum 4,000 cfs flow at each location). These travel times are used to dictate the forecast lead times needed to make decisions on reservoir operations and are used to evaluate precipitation and inflow forecast skill at Lake Mendocino.

Overall, this analysis suggests that there is sufficient confidence in the overall cool-season single and multi-day forecasted totals rainfall and inflow for Lake Mendocino within the timescales important for potential FIRO implementation. 24-hr precipitation forecasts had strong agreement to observations (R^2 exceeding 0.5) out to 4 days, while inflow forecasts showed strong agreement out through 5 days. Further analysis is needed to determine why the lead time skill of inflows is longer than precipitation in order to parse out the influence of land surface-based hydrologic processes (i.e. timescales of subsurface runoff into stream channel) versus implicit or underlying forecaster knowledge and skill. The longest lead time 72-hr and 120-hr combined forecasts capture between 81-88% of the variance of precipitation observations, which is indicative of both dry and wet periods. Ralph et al. 2019 showed that AR conditions in

northern California are observed approximately 12% of days out of the year; thus, the large variance explained often captures the skill of non-precipitating periods. However, these dry periods of the forecast will also be important for reservoir operations because they could potentially impact decisions on keeping water in the reservoir for future supply. Forecasts of no significant rainfall (i.e. less than 25.4 mm [1 inch] per day) were found to be quite skillful; underpredictions greater than 1 inch at 1-day lead time were quite rare (3 instances out of the 18-year period of record) and with the worst-case error of 76.5 mm (3.01 inches) on a 5-day lead time forecast. These types of errors were also shown to be rare on the basis of the forecast discrimination between a nominal event with precipitation below 25.4 mm (1 inch) and that predicted to be greater than 76.2 mm (3 inches). Up to a 4-day lead time, there is a better likelihood that forecasts can accurately discriminate between these two ends of the precipitation spectrum, leaving decision makers with more confidence in the overall qualitative forecast.

Absolute errors of extreme events of precipitation and inflow remain a challenge in this region. Lead-time errors in 24-hr precipitation can as large as 7-15% of the annual total of precipitation over the watershed. On average, the 72-hr and 120-hr forecasts of extreme events were most often high biased while forecasts of actual observed extreme events were low biased. There is a weak relationship between the magnitude of the extreme event and its forecast error that does not improve with increasing sample size (e.g. including events or forecasts with return periods less than 2-years). The additional water volume resulting from a missed 120-hr forecast of precipitation is estimated to be 7.9×10^6 m^3 (6400 ac-ft) per 25.4 mm (1 inch) of over-forecasted error and 2.2×10^6 m^3 (1800 ac-ft) per 25.4 mm (1 inch) under-forecasted error. At times, forecast errors of inflow can exceed 1.23×10^7 m^3 to 1.85×10^7 m^3 (10,000-15,000 ac-ft) over a 5-day period. Operations based on forecasts that overestimate the inflow could release too much water ahead of an ultimately weaker atmospheric river event, whereas under-forecasted inflows of stronger, longer duration atmospheric rivers could result in more accumulated water than was released from the reservoir.

Assuming a FIRO-run reservoir might reduce the flood pool by 1.23×10^7 m^3 to 1.48×10^7 m^3 (10-12,000 ac-ft), there is still over 3.7×10^7 - 1.23×10^7 m^3 (30,000 ac-ft) of flood pool in the reservoir. Thus, there are scenarios in which these forecast errors may be manageable using a FIRO modified

WCM. Additional reservoir modeling, testing, and evaluation is necessary to clearly define the risk associated with modulating the flood pool as a function of short-term precipitation and inflow forecasts. Ultimately, the degree in which FIRO can improve water supply and flood risk is a function of the forecast skill and the tools that leverage skill. Given that the extreme precipitation and inflow errors are largely associated with atmospheric rivers (i.e. each of the 120-hr forecast or observed events exceeding a 2-yr return period were associated with a land-falling atmospheric river), research in this area should focus on improved atmospheric river forecasts of location, timing, intensity and duration for 1 to 5-day lead times and the decision models that can leverage this improved skill. For example, ARs with properly modeled intensity but slight deviations in landfall location (on scales the size of a watershed) can significantly alter the overall precipitation and inflow skill of reservoir inflow areas. It is important to understand the overall predictability of the synoptic and mesoscale processes that control and evolve the vapor transport over localized regions for hydrologic applications.

Properly implemented, FIRO represents a potential solution for improving reservoir management outcomes for all authorized purposes without incurring expensive structural investments. The evaluation of forecast skill described herein provides a foundational basis for applying FIRO-like operations as well as guidance on areas in which forecasting for Lake Mendocino can be improved.

7 References

Benjamin, S.G., J.M. Brown, G. Brunet, P. Lynch, K. Saito, and T.W. Schlatter, 2018: 100 Years of Progress in Forecasting and NWP Applications. *Meteorological Monographs,* **59**, 13.1–13.67, https://doi.org/10.1175/AMSMONOGRAPHS-D-18-0020.1

Biswas, A. K., 2004: Integrated Water Resources Management: A Reassessment. *Water International*, **29(2)**, 248–256. http://doi.org/10.1080/02508060408691775

Brown, J. D., Wu, Limin, He, Minxue, Regonda, Satish, Lee, Haksu, Seo, Dong-Jun, 2014: Verification of temperature, precipitation, and streamflow forecasts from the NOAA/NWS Hydrologic Ensemble Forecast Service (HEFS): 1. Experimental design and forcing verification, *J. Hydrol.*, **519**, 2869–2889.

Butts, M. B., J. T. Payne, M. Kristensen, and H. Madsen, 2004: An evaluation of the impact of model structure on hydrological modeling uncertainty for streamflow simulation. *J. Hydrol.,* **298**, 242—266.

Charba, J. P., D. W. Reynolds, B. E. McDonald, and G. M. Carter, 2003: Comparative verification of recent quantitative precipitation forecasts in the National Weather Service: A simple approach for scoring forecast accuracy. *Wea. Forecasting*, **18**, 161–183.

Cherubini, T., A. Ghelli, and F. Lalaurette, 2002: Verification of precipitation forecasts over the Alpine region using a high-density observing network. *Wea. Forecasting*, **17**, 238–249.

Cordeira, J.M., F.M. Ralph, A. Martin, N. Gaggini, J.R. Spackman, P.J.Neiman, J.J. Rutz, and R. Pierce, 2017: Forecasting Atmospheric Rivers during CalWater 2015. Bull. Amer. Meteor. Soc., **98**, 449-459.

Cuo, L., T. C. Pagano, Q. J. Wang, 2011: A review of quantitative precipitation forecasts and their use in short- to medium-range streamflow forecasting. *J. Hydromet.* **12**, 713-728, doi:10.1175/2011JHM1347.1

Daly, C., R. P. Neilson, and D. L. Phillips, 1994: A statistical–topographic model for mapping climatological precipitation over mountainous terrain. *J. Appl. Meteor.*, **33**, 140–158.

Demargne, J. and others, 2014: The science of NOAA's Operational Hydrologic Ensemble Forecast Service. *Bull, Amer. Meteor. Soc.,* **95**, 79-98.

Dettinger, M., 2011: Climate change, atmospheric rivers, and floods in California – A multi-model analysis of storm frequency and magnitude changes. *J. Amer. Water Resour. Assoc.*, **47,** 514-523, doi:101111/j.1752-1688.2011.00546.x.

Dettinger, M., and Coauthors 2012: Design and quantification of an extreme winter storm scenario for emergency preparedness and planning exercises in California. Nat. Hazards, **60**, 1085\u20131111.

Glahn, Harry R., David P. Ruth, 2003: The New Digital Forecast Database of the National Weather Service. *Bull. Amer. Meteor. Soc.*, **84**, 195–201. doi: http://dx.doi.org/10.1175/BAMS-84-2-195

Forecast Informed Reservoir Operations Steering Committee. (2017). *Preliminary viability assessment of Lake Mendocino*. Available from http://escholarship.org/uc/item/66m803p2

Franz, K. J., and T. S. Hogue, 2011: Evaluating uncertainty estimates in hydrologic models: Borrowing measures from the forecast verification community, *Hydrology and Earth, System Sciences,* **15(11),** 3367–3382.

Henkel, A., and C. Peterson, 1996: Can deterministic quantitative precipitation forecasts in mountainous regions be specified in a rapid, climatologically-consistent manner with Mountain Mapper functioning as the tool for mechanical specification, quality control, and verification? *Abstracts, Fifth National Heavy Precipitation Workshop,* State College, PA, NWS/NOAA, 31 pp. [Available from Office of Climate, Water, and Weather Services, W/OS, 1325 East West Hwy., Silvery Spring, MD 20910].

Hoff, H., 2009:. Global water resources and their management. *Current Opinion in Environmental Sustainability*. http://doi.org/10.1016/j.cosust.2009.10.001

Jolliffe, I. T., and D. B. Stephenson, 2003: *Forecast Verification: A Practitioner's Guide in Atmospheric Science*. John Wiley and Sons, 254 pp.

Leung, L. R., and Y. Qian, 2009: Atmospheric rivers induced heavy precipitation and flooding in the western U.S. simulated by the WRF regional climate model. *Geophys. Res. Lett.*, **36**, L03820, doi:10.1029/2008GL036445.

Lund, J. R., and R. N. Palmer, 1997: Water Resource System Modeling for Conflict Resolution. *Water Resources Update*, ***3*,** 70–82.

Lund, J. R., 2015: Integrating social and physical sciences in water management. *Water Resources Research*, **51(8),** 5905–5918. http://doi.org/10.1002/2015WR017125

Mason, I., 1989: Dependence of the critical success index on sample climate and threshold probability. *Aust. Meteor. Mag.,* **37**, 75–81.

Mason, I. B., 2003: Binary Events. In: Forecast verification – a practitioner's guide in atmospheric science, (eds I. T. Jolliffe and D. B. Stephenson) Wiley, 240 pp.

Christian-Smith, J., and A. M. Merenlender, 2010: The disconnect between restoration goals and practices: A case study of watershed restoration in the Russian River basin, California. *Restoration Ecology*, **18(1)**, 95–102. http://doi.org/10.1111/j.1526-100X.2008.00428.x

Neiman, P. J., F. M. Ralph, G.A. Wick, Y.-H.Kuo,T.-K.Wee, Z.Ma, G.H.Taylor, and M. Dettinger, 2008a: Diagnosis of an intense atmospheric river impacting the Pacific Northwest: Storm summary and offshore vertical structure observed with COSMIC satellite retrievals. Mon. Wea. Rev.,**136**, 4398-4420.

Neiman, P. J., F. M. Ralph, G. A. Wick, J. D. Lundquist, and M. D. Dettinger, 2008b: Meteorological characteristics and overland precipitation impacts

of atmospheric rivers affecting the west coast of North America based on eight years of SSM/I satellite observations. *J. Hydrometeor*, **9**, 22–47.

Neiman, P. J., F. M. Ralph, B. J. Moore, M. Hughes, K. M. Mahoney, J. M. Cordeira, and M. D. Dettinger, 2013: The landfall and inland penetration of a flood-producing atmospheric river in Arizona. Part I: Observed synoptic-scale, orographic, and hydrometeorological characteristics. *J. Hydrometeor*, **14**, 460–484.

Neiman, P. J., B.J. Moore, A.B. White, G.A. Wick, J. Aikins, D.L. Jackson, J.R. Spackman, and F. M. Ralph, 2016: An airborne and ground-based study of a long-lived and intense atmospheric river with mesoscale frontal waves impacting California during CalWater-2014. *Mon. Wea. Rev.*, **144**, 1115-1143.

Nelson, B.R., O.P. Prat, D.J. Seo, and E. Habib, 2016: Assessment and implications of NCEP Stage IV quantitative precipitation estimates for product intercomparisons. *Wea.and Fcst.*, **31**, 371-394.

Novak, D.R., F.E. Barthold, M.J. Bodner, K.F. Brill, and M. Eckert, 2011: Quantifying extreme rainfall threats at the Hydrometeorological Prediction Center. *91st Amer. Meteor. Soc. Ann. Mtg,* Seattle, WA, AMS. [Available online at https://ams.confex.com/ams/91Annual/webprogram/24WAF20NWP.html]

Novak, D. R., C. Bailey, K. F. Brill, P. Burke, W. A. Hogsett, R. Rausch, M. Schichtel, 2014: Precipitation and temperature forecast performance at the Weather Prediction Center. *Wea. Forecasting*, **29**, 489-504.

Olson, D. A., N. W. Junker, and B. Korty, 1995: Evaluation of 33 years of quantitative precipitation forecasting at the NMC. *Wea. Forecasting*, **10**, 498–511.

Opperman, J., K. Lohse, C. Brooks, N. M. Kelly, A. M. Merenlender, 2005: Influence of land use on fine sediment in salmonid spawning gravels with the Russian River Basin, California. *Canadian J. Fisheries and Aquatic Science,* **62(12),** 61-73**,** doi:10.1139/f07-140

Pappenberger, F., J. Thielen, and M. Del Medico, 2011: The impact of weather forecast improvements on large scale hydrology: Analysing a decade of forecasts of the European Flood Alert System, *Hydrological Processes,* **25(7),** 1091–1113, doi:10.1002/hyp.7772.

Ralph, F.M., P.J.Neiman, and G. A. Wick, 2004: Satellite and CALJET observations of Atmospheric Rivers over the North Pacific during the winter of 1997/98. Mon. Wea. Rev. **132,** 1721-1745**.**

Ralph, F. M., and Coauthors, 2005: Improving short-term (0–48 h) cool-season quantitative precipitation forecasting: Recommendations from a USWRP Workshop. *Bull. Amer. Meteor. Soc.*, **86**, 1619–1632.

Ralph, F. M., P. J. Neiman, G. A. Wick, S. I. Gutman, M. D. Dettinger, D. R. Cayan, and A. B. White, 2006: Flooding on California's Russian River: Role of atmospheric rivers. *Geophys. Res. Lett.,* **33**, L13801, doi:10.1029/2006GL026689.

Ralph, F. M., E. Sukovich, D. Reynolds, M. Dettinger, S. Weagle, W. Clark, and P. J. Neiman, 2010: Assessment of extreme quantitative precipitation forecasts and development of regional extreme event thresholds using data from HMT-2006 and COOP observers. *J. Hydrometeor*, **11**, 1286–1304.

Ralph, F. M., P. J. Neiman, G.N. Kaladis, K. Weickman, and D.W. Reynolds, 2011: A multi-scale observational case study of a Pacific atmospheric river exhibiting tropical-extratropical connections and a mesoscale frontal wave. *Mon. Wea. Rev.*, **139**, 1169-1189.

Ralph, F. M., and M. D. Dettinger, 2012: Historical and national perspectives on extreme west coast precipitation associated with atmospheric rivers during December 2010. *Bull. Amer. Meteor. Soc.*, **93**, 783–790.

Ralph, F. M., T. Coleman, P. J. Neiman, R. J. Zamora, and M. D. Dettinger, 2013: Observed impacts of duration and seasonality of atmospheric-river landfalls on soil moisture and runoff in coastal northern California. *J. Hydrometeor*, **14**, 443–459.

Ralph, F.M., J.J. Rutz, J.M. Cordeira, M. Dettinger, M. Anderson, D. Reynolds, L.J. Schick, and C. Smallcomb, 2019: A Scale to Characterize the

Strength and Impacts of Atmospheric Rivers. *Bull. Amer. Meteor. Soc.,* **100**, 269–289, https://doi.org/10.1175/BAMS-D-18-0023.1

Reynolds, D. W., 2003: Value-added quantitative precipitation forecasts: How valuable is the forecaster? *Bull. Amer. Meteor. Soc.*, **84**, 876–878.

Rutz, J.J., W.J. Steenburgh, F. M. Ralph, 2014, Climatological characteristics of atmospheric rivers and their inland penetration over the Western United States. *Mon. Wea. Rev.*, **142**, 905-921.

Sellars, S.L., X Gao, S. Sorooshian, 2015: An Object-Oriented Approach to Investigate Impacts of Climate Oscillations on Precipitation: A Western United States Case Study. *J Hydrometeor.*, **16(2),** 830–842.

Schumacher, R. S., and C. A. Davis, 2010: Ensemble-based forecast uncertainty analysis of diverse heavy rainfall events. *Wea. Forecasting*, **25**, 1103–1122.

Smith, B. L., S. E. Yuter, P. J. Neiman, and D. E. Kingsmill, 2010: Water vapor fluxes and orographic precipitation over northern California associated with a land-falling atmospheric river. *Mon. Wea. Rev.,* **138**, 74\u2013100.

Sukovich, E. M., F. M. Ralph, F. Barthold, D. W. Reynolds, D. R. Novak, 2014: Extreme Quantitative Precipitation Forecast Performance at the Weather Prediction Center from 2001 to 2011. *Wea. Forecasting, **29**,* 894-911.

Werner, M., J. Schellekens, P. Gijsbers, M. van Dijk, O. van den Akker, and K. Heynert (2013), The Delft-FEWS flow forecasting system, Environmental Modelling and Software, **40**, 65–77, doi:10.1016/j.envsoft.2012.07.010.

White, A. B., and Coauthors, 2012: NOAA's rapid response to the Howard A. Hanson Dam flood risk management crisis. *Bull. Amer. Meteor. Soc.*, **93**, 189–207.

Wick, G. A., P. J. Neiman, F. M. Ralph, and T. M. Hamill, 2013: Evaluation of forecasts of the water vapor signature of atmospheric rivers in operational numerical weather prediction models. *Wea. Forecasting*, **28**, 1337\u20131352, doi:10.1175/WAF-D-13-00025.1.

Yang, T., X. Gao, S. L. Sellars, and S. Sorooshian, 2015: Improving the multi-objective evolutionary optimization algorithm for hydropower reservoir operations in the California Oroville–Thermalito complex. *Environmental Modelling & Software*, **69**, 262-279.

Yang, T., X. Gao, S. Sorooshian, and X. Li, 2016: Simulating California reservoir operation using the classification and regression-tree algorithm combined with a shuffled cross-validation scheme. *Water Resources Research*, **52(3),** 1626-1651.

Appendix: Acronyms

Acronym	Meaning
CHPS	Community Hydrologic Prediction System
CNRFC	California Nevada River Forecast Center
CVD	Coyote Valley Dam
CW3E	Center for Western Weather and Water Extremes
FIRO	Forecast-informed Reservoir Operations
FIRO-AF	FIRO Assessment Framework
GFE	Graphical Forecast Editor
HAS	Hydrometeorological Analysis and Support
HRAP	Hydrologic Rainfall Analysis Project
MAP	Mean Areal Precipitation
MERRA	Modern-Era Retrospective analysis for Research and Applications
NCEP	National Centers for Environmental Prediction
NOAA	National Oceanic and Atmospheric Administration
NWS	National Weather Service
PRISM	Parameter-elevation Regressions on Independent Slopes Model
PVA	Preliminary Viability Assessment
QPF	Quantitative Precipitation Forecast
QPE	Quantitative Precipitation Estimate
SCWA	Sonoma County Water Agency
UCSD	University of California, San Diego
USACE	US Army Corps of Engineers
WCM	Water Control Manual
WFO	Weather Forecast Office

WPC	Weather Prediction Center